Communication

Facile fabrication of nickel nanostructures via galvanic replacement reaction in a deep eutectic solvent

C. Yang[a], Q. B. Zhang[a*] , and Andrew P. Abbott[b]

[a] Key Laboratory of Ionic Liquids Metallurgy, Faculty of Metallurgical and Energy Engineering, Kunming University of Science and Technology. Kunming, 650093, P.R. China

[b] Department of Chemistry, University of Leicester, Leicester, LE1 7RH, UK

Abstract

We describe an unusual galvanic replacement process for facile synthesis of nickel nanostructures by using Cu as a sacrificial template in a deep eutectic solvent (DES) Ethaline. This replacement process occurred through a Galvanic exchange of $[NiCl_4]^{2-}$ ions in Ethaline at 353 K with an immersed Cu substrate, which acted as both reactive template and reductant. The mechanism for this replacement reaction and the morphology and topography evolution process of nickel nanostructures were investigated. This facile preparation method performed in Ethaline provides a novel way to fabricate nickel nanostructures on the copper-based template.

Keywords : Copper; Nickel nanostructures; Nanoporous; Deep eutectic solvent; Galvanic replacement reaction

* Corresponding author. Tel: +86-871-65162008; fax: +86-871-65161278.

E-mail address: qibozhang@kmust.edu.cn (Q.B. Zhang)

1. Introduction

Galvanic replacement reactions have been shown to be capable of preparing metallic nanostructures, particularly for nanocrystals with hollow and core-shell nanoarchitectures.[1-3] In general, a sacrificial metal substrate can be treated as a reactive template with a suitable metal salt, whose redox potential should be higher than that of the template material.[4,5] Compared to electrodeposition and electroless processes, galvanic replacement approach is easier to operate and control, since no additional substances, such as additives, reducing agents, complexants, buffers, and accelerators are involved.[6]

Conventional replacement reactions are mostly confined to aqueous solutions, where various aspects including speciation, reaction mechanism, kinetic control and resultant structure tuning have been extensively investigated.[7-10] Ionic liquids (ILs) have recently become attractive media for fabrication of metallic nanostructures by the galvanic replacement strategy.[11-13] ILs are generally aprotic with relatively high viscosity and provide a different chemical environment compared to molecule solutions. Unusual single-crystalline dendritic Au[11] and Au-Ag[12,13] nanostructures with high catalytic activity have been observed. Deep eutectic solvents (DESs), are mixtures of quaternary ammonium salts and hydrogen bond donors[14,15] and provide potential alternatives to conventional ILs. Porous silver films were self-assembled by simple galvanic replacement reactions from the choline chloride (ChCl)-based DES.[16,17] It was found that by modulating reaction conditions, nanoporous Ag films with super hydrophobic properties could be obtained on a copper alloy substrate.[18] The intriguing solvent properties of DESs such as polarity, surface tension, and highly ordered hydrogen bonding, potentially provide an environment for the generation of nanostructured materials.[19-21] Moreover, the capacity to tune redox properties in DESs[22] enables the possibility to obtain Galvanic exchange processes that are difficult to realize in aqueous solutions.

In this communication, we report that nickel nanostructures can be fabricated via galvanic replacement of a copper template in the DES Ethaline. This is an unusual finding as nickel (E^0 = -0.257 V. vs SHE) cannot normally be deposited onto copper (E^0 = 0.34 V. vs SHE)[23] without chemical reducing agents. This is the first time that copper has been replaced with nickel by a galvanic replacement reaction. This study also investigates the reaction mechanism in Ethaline.

2. Experimental

Choline chloride (ChCl, Aldrich, 98%), ethylene glycol (EG) (Aldrich, 99.5%), $CuCl_2 \cdot 2H_2O$ (Aldrich, 99.5%), and $NiCl_2 \cdot 6H_2O$ (Aldrich, 99.5%) were used as-received. Ethaline was prepared by mixing the components in the molar proportion of 1 ChCl: 2 EG according to the method in ref 24.

Cyclic voltammetric (CV) experiments were conducted in an open system in a conventional three-electrode cell made of glass using a CHI 760D electrochemical working station. A 2 mm diameter Pt working electrode, a Pt counter electrode and a 1 mm diameter Ag wire (10 mm in length) reference electrode were used. Galvanic replacement experiments were performed in vials with 20 mL 0.10 M $NiCl_2 \cdot 6H_2O$ containing Ethaline at 353 K. Samples and solvents at different stages of the reaction were taken for characterization.

The as-prepared samples were rinsed with anhydrous alcohol followed by distilled water, air dried and analyzed directly by scanning electron microscopy (SEM, HITACHI S-3400N), X-ray diffraction spectroscopy (XRD, SHIMADZU X-ray 6000 with Cu-Ka), X-ray photoelectron spectroscopy (XPS, PHI 5000 Versa-Probe), and atomic force microscopy (AFM, Dimension 3100). UV–VIS spectra of the resultant solutions were determined at room-temperature by diluting samples to a concentration of 0.1 mM and measuring in a 1 cm path length quartz cuvette with a Varian Cary 50 UV–VIS spectrophotometer. The nanoporous copper (NPC) templates used were prepared as reported previously[25] and the resultant samples were characterized by transmission electron microscopy (TEM, JEOL JEM-2010F).

3. Results and discussion

Cyclic voltammograms (CVs) for the redox behavior of copper and nickel on a Pt electrode from Ethaline containing 0.10 M $CuCl_2 \cdot 2H_2O$ and 0.10 M $NiCl_2 \cdot 6H_2O$, respectively, at 353 K are presented in Fig. 1a. Two well defined redox couples (Cu^{II}/Cu^{I} and Cu^{I}/Cu^{0}) can be observed, which has been studied previously at room temperature.[22] For nickel, a single Ni^{II}/Ni^{0} redox couple is obtained. It is notable that the redox potential for Cu^{I}/Cu^{0} (-0.350 V) in Ethaline is ca. 200 mV more negative than that of Ni^{II}/Ni^{0} (-0.154 V), determined by the average of onset potentials (E_{ca}, E_{oa}) and (E_{cb}, E_{ob}) respectively.[20] This result indicates that a galvanic replacement reaction of copper with nickel is thermodynamically feasible in Ethaline at 353 K. To confirm this a copper substrate was immersed in Ethaline with 0.10 M $NiCl_2 \cdot 6H_2O$ for 5 h at 353 K and a thin, well-adhering film with a silvery metallic-like deposit was obtained (Fig.1b). SEM analysis shows that the flat copper surface was transformed to a rougher surface filled with nanoparticles and cracks after reaction with the Ni^{II} species.

The X-ray diffraction (XRD) pattern for the resultant deposit is shown in Fig.1c. The corresponding diffraction peaks centered at 43.6, 50.6, and 74.3°, that are located between the standard Cu (JCPDS Card No. 04-0836) and Ni (JCPDS Card No. 65-0380). Although it is difficult to assign the peaks unequivocally to Cu/Ni as they have very similar lattice parameters,[8] the shift of the diffraction peaks towards those for Ni after the replacement reaction can be attributed to the partial replacement of Cu atoms with Ni atoms, which causes a decrease in the lattice parameters.[26]

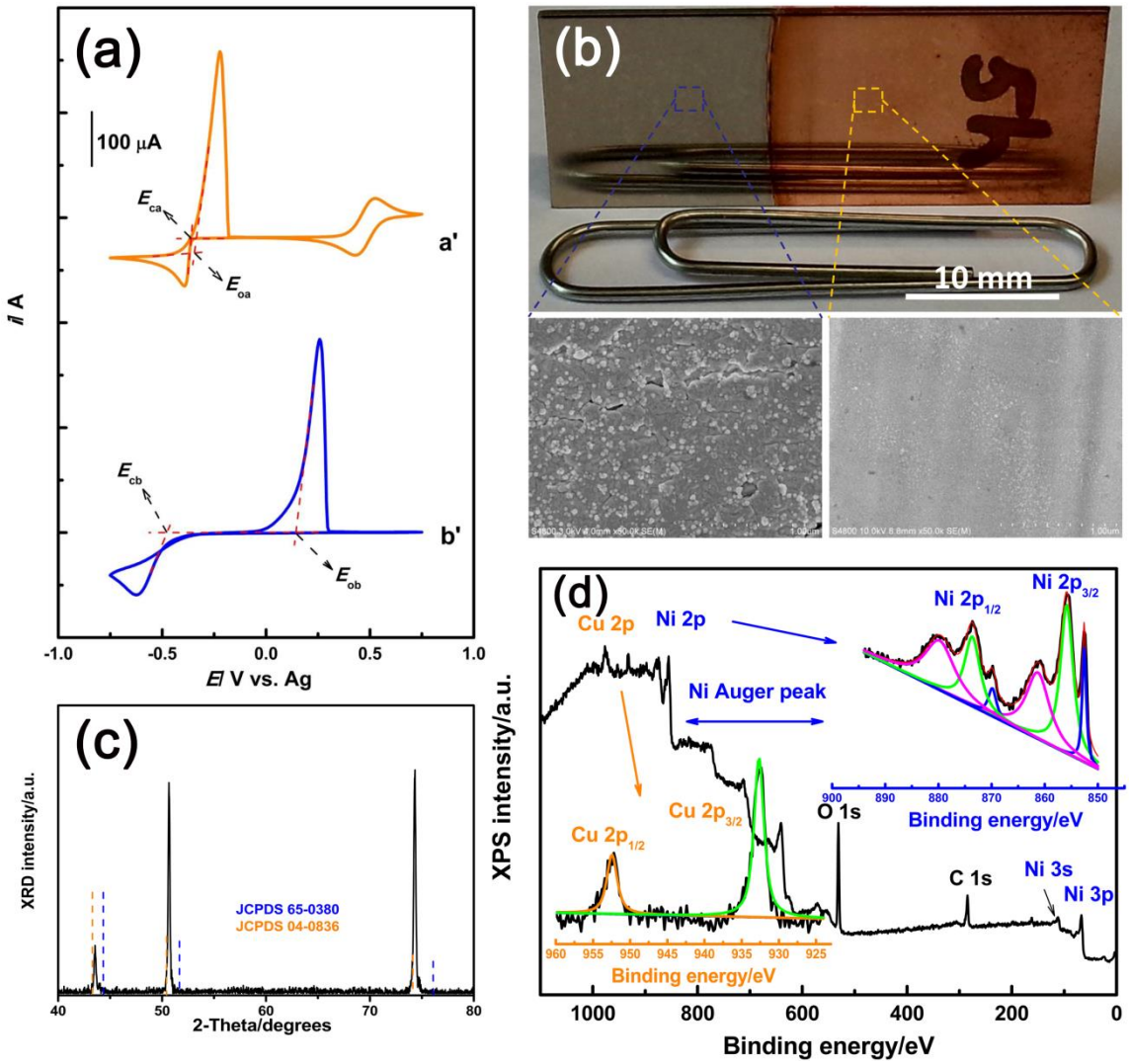

Fig. 1. (a) CVs of 0.10 M $CuCl_2{\cdot}2H_2O$ (a') and 0.10 M $NiCl_2{\cdot}6H_2O$ (b') in Ethaline recorded at Pt electrode, respectively. Scan rate: 10 mV/s. Temperature: 353 K. (b) Photographic image for Cu foil before and after replacement for 5 h in 0.10 M $NiCl_2{\cdot}6H_2O$/Ethaline at 353 K, and corresponding SEM analysis. (c) XRD pattern of the prepared Ni/Cu sample: The standard patterns of pure Ni (blue, JCPDS 65-0380) and Cu (orange, JCPDS 04-0836) are attached for comparison. (d) XPS survey spectra of the Ni loaded Cu foil, and the corresponding Cu2p and Ni2p XPS spectra analysis.

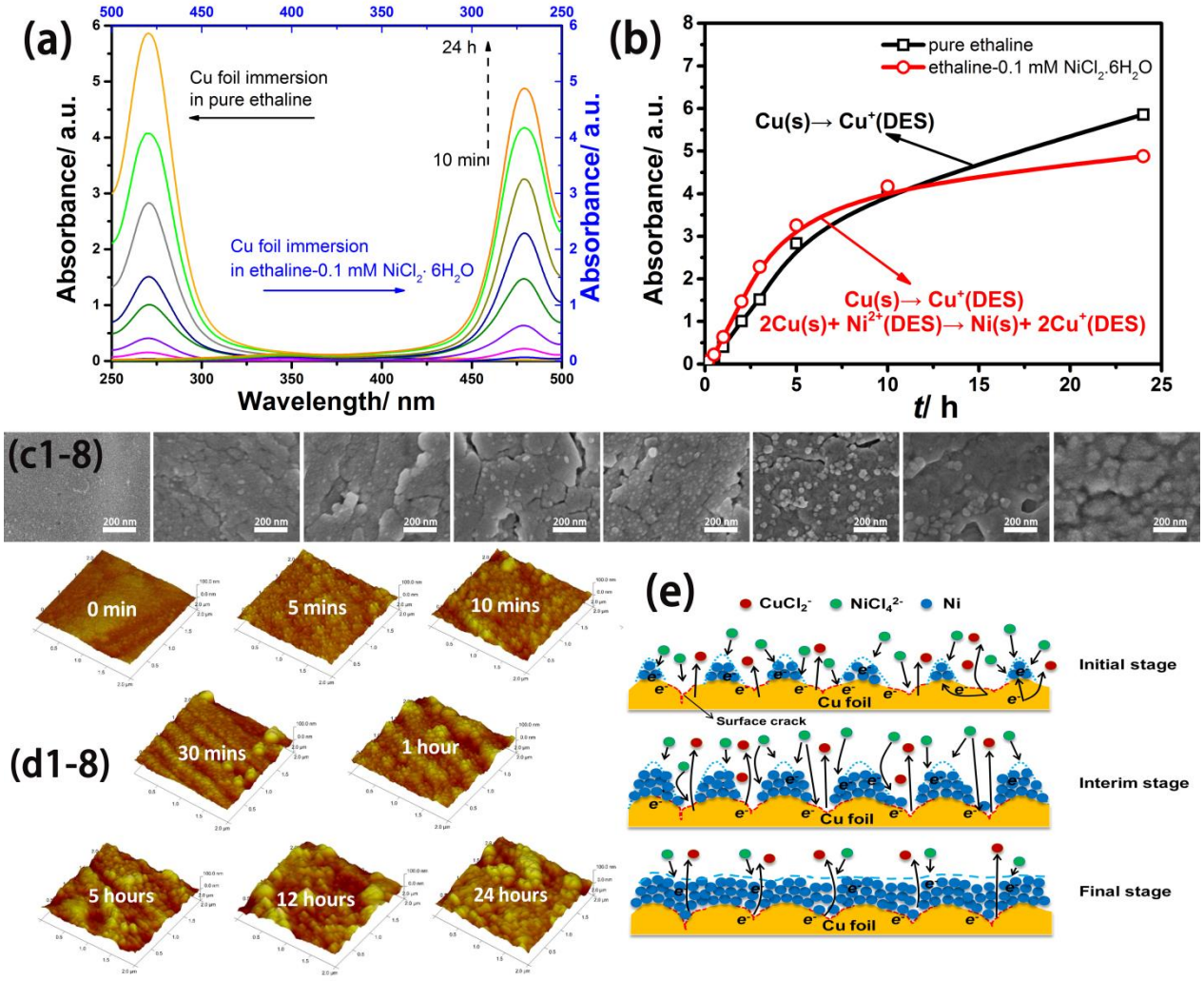

Fig.2. (a) UV-vis spectra of pure Ethaline and Ethaline containing $NiCl_2 \cdot 6H_2O$ after different stages of replacement. (b) Comparison of absorbance at 270 nm as a function of reaction time. (c1-8) SEM images showing the morphological changes of the Ni-modified Cu foil, and their corresponding (d1-8) AFM images at various stages of replacement. (e) Schematic illustration of structure evolution of the Ni-modified Cu foil.

In addition, the surface chemical states of the deposit were further revealed by XPS, as shown in Fig.1d. Peaks in the full XPS spectrum correspond to Cu, Ni, O, and C. Detection of O is most likely due to a surface reaction of the freshly deposited products, and the presence of C comes mainly from the solvent residue. Curve fitting of the Cu 2p and Ni 2p XPS signals (inserts in Fig. 1d) give single metallic copper (932.7 and 952.4 eV) with different nickel species. The principle doublet peaks at 852.6 and 869.9 eV correspond to metallic nickel. The peaks at 855.8 and 873.6 eV can be assigned to Ni^{II} species such as NiO. It is clear that the Ni 2p spectrum shows a complex structure with intense satellite peaks of c.a. 6 eV higher binding energy (BE) adjacent to the Ni $2p_{3/2}$ and $2p_{1/2}$ peaks (855.8 and 873.6 eV, respectively), which can be ascribed to a multi-electron excitation. The corresponding shake-up peaks observed at 861.3 and 879.8 eV also belong to Ni^{II} species. This result reveals that the top surface of the deposit mainly consists of metallic Ni and NiO, which corresponds well with the TEM analysis (Fig. 3c and d).

As obtained above, the c.a. 200 mV differences of the redox potentials between Cu^{I}/Cu^{0} and Ni^{II}/Ni^{0} at 353K can readily drive a spontaneous galvanic-replacement reaction. The Cu foil can serve as a template for the reaction, being oxidized by the Ni^{II} species in Ethaline as $[NiCl_4]^{2-}$ ions[27] according to:

$2Cu(s) + Ni^{II}(DES) \rightarrow Ni(s) + 2Cu^{I}(DES)$.

The concentration of $[CuCl_3]^{2-}$ ions (270 nm) generated in Ethaline,[28,29] is observed to increase with increasing reaction time according to the UV-vis absorption spectra (Fig. 2a). Etching the Cu substrate through anodic polarisation is also found to form $[CuCl_3]^{2-}$ ions in pure Ethaline at 353 K, however, the corresponding absorbance is smaller than that for the $NiCl_2{\cdot}6H_2O$-containing case, particularly in the early stage, which confirms the occurrence of atomic replacement as indicated. The coverage of the copper substrate with Ni islands will hinder the interface reaction through decreased mass transfer due to blocking which causes the absorbance to level off (Fig. 2b).

To gain further insight into the deposition methodology the morphological and topographical changes at various stages was characterized using SEM and AFM analysis. Fig.2c (1-8) shows the morphological evolution of the Ni-modified Cu foil. After the Cu foil initially contact with Ni^{II} complex in Ethaline (5 mins), surface cracks are gradually formed, resulting in a rough and locally porous surface. This effect becomes more pronounced at longer immersion times (1 h). The resultant surface cracks should be derived from the stripping of Cu substrate, which release electrons and drive the replacement reaction. The reduction of Ni^{II} species is initiated at the exposed terrace regions of the substrate surface and results in the formation of nanoparticles. As the reaction proceeds, the uncovered porous surfaces continue to enable Cu to be oxidized to $[CuCl_3]^{2-}$. The generated electrons instantaneously migrate to the vacant sites or as-deposited Ni crystallites nearby and are captured by $[NiCl_4]^{2-}$ ions, generating Ni atoms that further grow on these active sites. This growth process can be seen with increasing immersion time from 1 to 12 h. As the Ni layer forms gradually, the exposed copper cracks/channels decrease in size, decreasing the rate of the dissolution process until the overlaying Ni networks is complete (24 h) where after growth is much slower until it eventually stops.

The time-resolved AFM images record the topographical changes of the Ni-modified Cu foils with more insight into the nucleation and growth of Ni nanostructures (Fig. 2d (1-8)). It suggests that the nucleation of Ni^{II} species occurs via a progressive mechanism as Ni crystallites with different sizes are clearly visible from the AFM images throughout the replacement period. The whole reaction process/structure evolution of the Ni-modified Cu foils occurs via three main stages, as shown in the schematic illustration in Fig. 2e. Initially (5-10 mins), Cu stripping results in a porous structure with surface cracks, which releases electrons for the deposition of Ni^{II} species with a progressive nucleation mechanism. As the reaction goes on, more Cu atoms are depleted with development of the surface cracks and the deposited Ni clusters gradually grow together to form a ridged structure (0.5-1 h). Moreover, the further growth of the deposited Ni atoms results in a decrease in the copper exposed until a flat Ni layer is obtained.

It should be noted that the deposition rate for this replacement process is rather slow in contrast to that in conventional aqueous solutions, even at a high temperature, which could be attributed to the sluggish

mass transfer in Ethaline with its relatively high viscosity. However, this slow replacement rate makes it easier to control the growth of metal nanostructures with high active surface areas.

Nanoparticulate nickel or 3D interconnected core/shell nanoporous nickel is an important catalytic material especially for the high hydrogen evolution reaction (HER)which is difficult to obtain by conventional routes.[30,31] Fig.3 shows that 3D interconnected core/shell nanoporous nickel can be fabricated by simple galvanic replacement in Ethaline with a nanoporous copper (NPC) template (Fig.3a). The resultant nanoporous nickel exhibits ultrahigh HER catalytic activity (Fig.3g) with a small Tafel slope of 58.5 mV dec^{-1} (Fig. 3h), which is comparable to those obtained for nanostructured nickel based HER catalysts in alkaline media, such as Ni-P nanoparticles loaded on Cu foam (55 mV dec^{-1}),[32] 3D ordered macro-/ mesoporous Ni (52 mV dec^{-1}),[33] and nanoscale NiO/Ni-CNT loaded on Ni foam (51 mV dec^{-1}).[34]

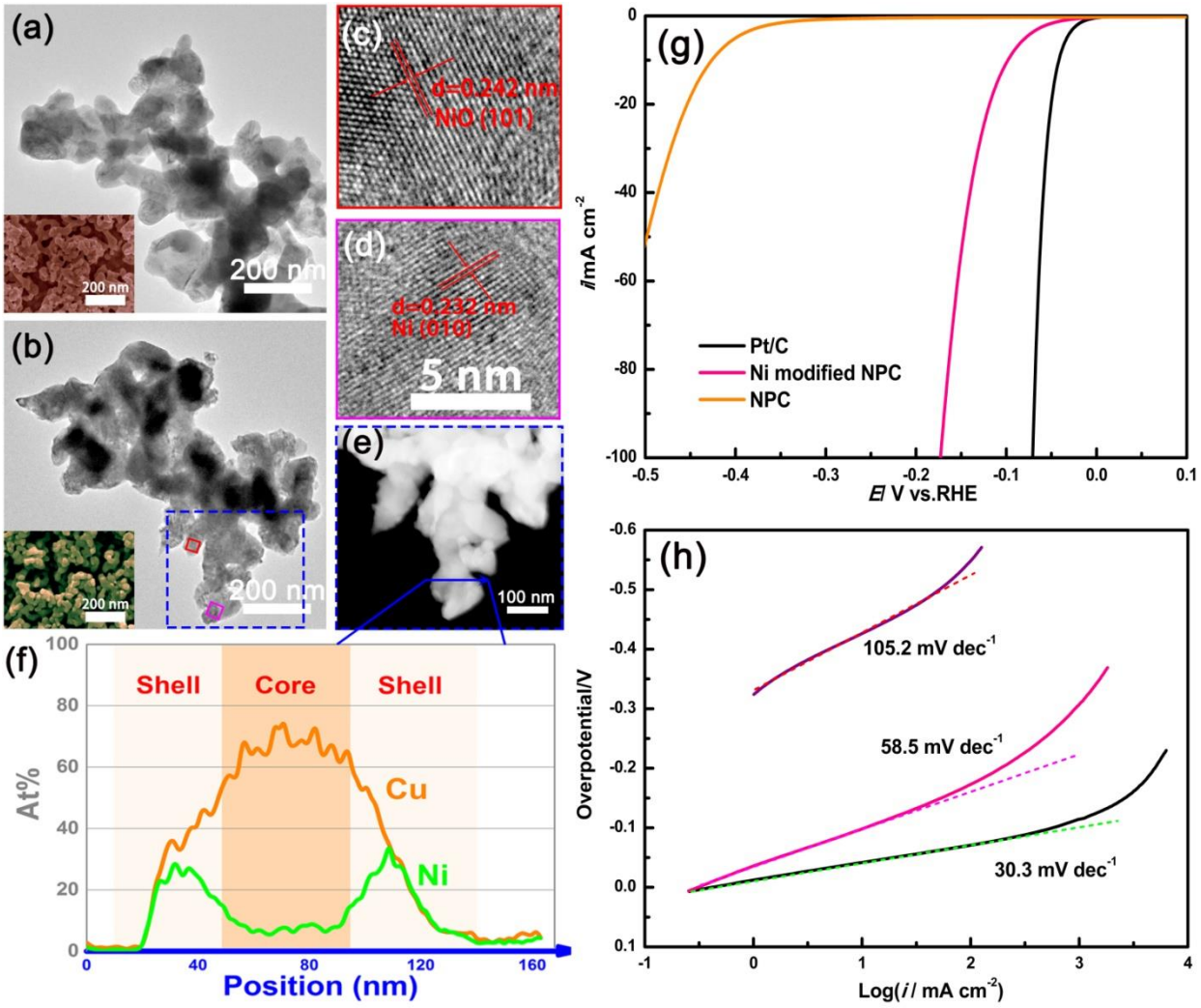

Fig.3. TEM micrographs of NPC (a) and Ni-modified NPC after replacement for 5 h at 353 K in 0.10 M $NiCl_2 \cdot 6H_2O$/ Ethaline (b). Insets: Corresponding SEM images. (c,d) High Revolution-TEM images, and (e) HAADF-STEM image of the selected region in (b) and a local elemental distribution for Cu and Ni along the ligament by STEM-EDS line profiles (f). (g) Polarization curves of Ni modified NPC and Pt/C (15 wt% Pt) electrodes in 1.0 M KOH at 298 K and a scan rate of 2 mV s^{-1}. (h) Corresponding Tafel plots with linear fitting.

4. Conclusion

Ni nanostructures were simply synthesized using galvanic replacement reaction in Ethaline containing $NiCl_2 \cdot 6H_2O$ at 353 K, using Cu as the sacrificial template. In this ionic system, the difference in redox potential for Cu^+/Cu^0 compared to that of Ni^{2+}/Ni^0 drives a spontaneous replacement reaction. Time-resolved studies reveal that the stripping of the copper substrate results in a porous surface and simultaneously initiates a progressive nucleation and growth of Ni nanoparticles, which gradually grow up by rearrangement of the Ni clusters to form flat nano-networks. The galvanic replacement method employed in DESs may open a facile way to synthesize nickel nanostructures with specific morphologies, for instance, nanoporous Ni with high HER catalytic activity using a NPC template, which are difficult to realize in conventional molecular solutions.

Acknowledgements

The authors gratefully acknowledge the financial support of the National Natural Science Foundation of China (5167010529, 51464028 and 51204080), and the Application Foundation Research of Yunnan Province (2014FB125).

References

[1] Y. Sun, Y. Xia, Shape-controlled synthesis of gold and silver nanoparticles, Science, 298 (2002) 2176-2179.

[2] Q. Zhang, J. Xie, J.Y. Lee, J. Zhang, C. Boothroyd, Synthesis of Ag@AgAu metal core/alloy shell bimetallic nanoparticles with tunable shell compositions by a galvanic replacement reaction, Small, 4 (2008) 1067-1071.

[3] E. González, J. Arbiol, V.F. Puntes, Carving at the nanoscale: Sequential galvanic exchange and Kirkendall growth at room temperature, Science, 334 (2011) 1377-1380.

[4] S.E. Skrabalak, J. Chen, Y. Sun, X. Lu, L. Au, C.M. Cobley, Y. Xia, Gold nanocages: synthesis, properties, and applications, Accounts of Chemical Research, 41 (2008) 1587-1595.

[5] L. Au, X. Lu, Y. Xia, A comparative study of galvanic replacement reactions involving Ag nanocubes and $AuCl_2^-$ or $AuCl_4^-$, Advanced Materials, 20 (2008) 2517-2522.

[6] P. Sahoo, S.K. Das, Tribology of electroless nickel coatings–a review, Materials & Design, 32 (2011) 1760-1775.

[7] Y. Yin, C. Erdonmez, S. Aloni, A.P. Alivisatos, Faceting of nanocrystals during chemical transformation: from solid silver spheres to hollow gold octahedra, Journal of the American Chemical Society, 128 (2006) 12671-12673.

[8] V. Bansal, H. Jani, J. Du Plessis, P.J. Coloe, S.K. Bhargava, Galvanic Replacement Reaction on Metal Films: A One-Step Approach to Create Nanoporous Surfaces for Catalysis, Advanced Materials, 20 (2008) 717-723.

[9] V. Bansal, A.P. O'Mullane, S.K. Bhargava, Galvanic replacement mediated synthesis of hollow Pt nanocatalysts: significance of residual Ag for the H_2 evolution reaction, Electrochemistry Communications, 11 (2009) 1639-1642.

[10] D. Zhao, Y.-H. Wang, B. Yan, B.-Q. Xu, Manipulation of Pt-Ag nanostructures for advanced electrocatalyst, The Journal of Physical Chemistry C, 113 (2009) 1242-1250.

[11] Y. Qin, Y. Song, N. Sun, N. Zhao, M. Li, L. Qi, Ionic liquid-assisted growth of single-crystalline dendritic gold nanostructures with a three-fold symmetry, Chemistry of Materials, 20 (2008) 3965-3972.

[12] A. Pearson, A.P. O'Mullane, V. Bansal, S.K. Bhargava, Galvanic replacement mediated transformation of Ag nanospheres into dendritic Au–Ag nanostructures in the ionic liquid [BMIM][BF_4], Chemical Communications, 46 (2010) 731-733.

[13] A. Pearson, A.P. O'Mullane, S.K. Bhargava, V. Bansal, Comparison of nanostructures obtained from galvanic replacement in water and an ionic liquid for applications in electrocatalysis and SERS, Electrochemistry Communications, 25 (2012) 87-90.

[14] A.P. Abbott, G. Capper, D.L. Davies, R.K. Rasheed, V. Tambyrajah, Novel solvent properties of choline chloride/urea mixtures, Chemical Communications, (2003) 70-71.

[15] A.P. Abbott, D. Boothby, G. Capper, D.L. Davies, R.K. Rasheed, Deep eutectic solvents formed between choline chloride and carboxylic acids: versatile alternatives to ionic liquids, Journal of the American Chemical Society, 126 (2004) 9142-9147.

[16] A.P. Abbott, S. Nandhra, S. Postlethwaite, E.L. Smith, K.S. Ryder, Electroless deposition of metallic silver from a choline chloride-based ionic liquid: a study using acoustic impedance spectroscopy, SEM and atomic force microscopy, Physical Chemistry Chemical Physics, 9 (2007) 3735-3743.

[17] A.P. Abbott, J. Griffith, S. Nandhra, C. O'Connor, S. Postlethwaite, K.S. Ryder, E.L. Smith, Sustained electroless deposition of metallic silver from a choline chloride-based ionic liquid, Surface and Coatings Technology, 202 (2008) 2033-2039.

[18] C. Gu, X. Xu, J. Tu, Fabrication and wettability of nanoporous silver film on copper from choline chloride-based deep eutectic solvents, The Journal of Physical Chemistry C, 114 (2010) 13614-13619.

[19] D.V. Wagle, H. Zhao, G.A. Baker, Deep eutectic solvents: Sustainable media for nanoscale and functional materials, Accounts of chemical research, 47 (2014) 2299-2308.

[20] Q.B. Zhang, Y.X. Hua, Electrochemical synthesis of copper nanoparticles using cuprous oxide as a precursor in choline chloride–urea deep eutectic solvent: nucleation and growth mechanism, Physical Chemistry Chemical Physics, 16 (2014) 27088-27095.

[21] Q.B. Zhang, A.P. Abbott, C. Yang, Electrochemical fabrication of nanoporous copper films in choline chloride–urea deep eutectic solvent, Physical Chemistry Chemical Physics, 17 (2015) 14702-14709.

[22] A. Abbott, G. Frisch, S. Gurman, A. Hillman, J. Hartley, F. Holyoak, K. Ryder, Ionometallurgy: designer redox properties for metal processing, Chemical Communications, 47 (2011) 10031-10033.

[23] A.J. Bard, R. Parsons, J. Jordan, Standard potentials in aqueous solution, CRC press, 1985.

[24] A.P. Abbott, G. Capper, D.L. Davies, R.K. Rasheed, P. Shikotra, Selective extraction of metals from mixed oxide matrixes using choline-based ionic liquids, Inorganic chemistry, 44 (2005) 6497-6499.

[25] C. Yang, Q.B. Zhang, M.Y. Gao, Y.X. Hua, C.Y. Xu, In-situ electrochemical fabrication of three dimension hierarchical nanoporous copper films and their electrocatalysis performance, Journal of The Electrochemical Society, Revision.

[26] Y. Fan, P.-F. Liu, Z.-W. Zhang, Y. Cui, Y. Zhang, Three-dimensional hierarchical porous platinum–copper alloy networks with enhanced catalytic activity towards methanol and ethanol electro-oxidation, Journal of Power Sources, 296 (2015) 282-289.

[27] A.P. Abbott, A. Ballantyne, R.C. Harris, J.A. Juma, K.S. Ryder, A Comparative Study of Nickel Electrodeposition Using Deep Eutectic Solvents and Aqueous Solutions, Electrochimica Acta, 176 (2015) 718-726.

[28] P. De Vreese, N.R. Brooks, K. Van Hecke, L. Van Meervelt, E. Matthijs, K. Binnemans, R. Van Deun, Speciation of copper (II) complexes in an ionic liquid based on choline chloride and in choline chloride/water mixtures, Inorganic Chemistry, 51 (2012) 4972-4981.

[29] D. Lloyd, T. Vainikka, L. Murtomäki, K. Kontturi, E. Ahlberg, The kinetics of the Cu^{2+}/Cu^{+} redox couple in deep eutectic solvents, Electrochimica Acta, 56 (2011) 4942-4948.

[30] C.Y. Cao, C.Q. Chen, W. Li, W.G. Song, W. Cai, Nanoporous nickel spheres as highly active catalyst for hydrogen generation from ammonia borane, ChemSusChem, 3 (2010) 1241-1244.

[31] J. Cai, J. Xu, J. Wang, L. Zhang, H. Zhou, Y. Zhong, D. Chen, H. Fan, H. Shao, J. Zhang, Fabrication of three-dimensional nanoporous nickel films with tunable nanoporosity and their excellent electrocatalytic activities for hydrogen evolution reaction, International Journal of Hydrogen Energy, 38 (2013) 934-941.

[32] Q. Liu, S. Gu, C.M. Li, Electrodeposition of nickel–phosphorus nanoparticles film as a Janus electrocatalyst for electro-splitting of water, Journal of Power Sources, 299 (2015) 342-346.

[33] T. Sun, C. Zhang, J. Chen, Y. Yan, A.A. Zakhidov, R.H. Baughman, L. Xu, Three-dimensionally ordered macro-/mesoporous Ni as a highly efficient electrocatalyst for the hydrogen evolution reaction, Journal of Materials Chemistry A, 3 (2015) 11367-11375.

[34] M. Gong, W. Zhou, M.-C. Tsai, J. Zhou, M. Guan, M.-C. Lin, B. Zhang, Y. Hu, D.-Y. Wang, J. Yang, Nanoscale nickel oxide/nickel heterostructures for active hydrogen evolution electrocatalysis, Nature communications, 5 (2014).